Research Article

Ying Guo and Shi Yan*

Experimental investigation on compressive properties of three-dimensional five-directional braided composites in hygrothermal environment

https://doi.org/10.1515/secm-2022-0153 received May 23, 2022; accepted August 30, 2022

Abstract: This article describes work concerning the compressive properties in hygrothermal environment of three-dimensional (3D) five-directional braided composites. Hygrothermal aging tests at temperatures of 40, 60, and 80°C and compression tests were carried out on the specimens with three braiding angles of 15, 25, and 35°. The surface morphologies of the samples taken using scanning electron microscope before and after the hygrothermal aging test were used to analyze the influence of the hygrothermal environment on the internal structure of braided composites. The experimental results indicate that the hygrothermal environment has a more influence on the specimens with a braiding angle of 15°, and the greater the moisture absorption percentage, the lower the retention ratios of compressive strength and modulus. Compared with room temperature, the compressive strength and modulus of specimens with a braiding angle of 15° reduced by 72.2 and 82.7% as the water bath temperature increased from 40 to 80°C. Moreover, the failure mechanisms of 3D five-directional braided composites in the hygrothermal environment were analyzed.

Keywords: 3D five-directional braided composites, hygrothermal aging test, moisture absorption percentage, compressive strength, compressive modulus

Ying Guo: Department of Engineering Mechanics, Harbin University of science and Technology, Harbin, China

International License.

1 Introduction

Fiber-reinforced composites have been used widely in the fields of astronautics, aeronautics, military, and construction because of distinct advantages of high specific strength and modulus, excellent fatigue resistance, and seismic resistance [1-4]. Composites may be exposed to hygrothermal environments in the process of use, such as drilling platforms at sea, aircraft and vehicles parked in hot and humid climate conditions, and filling materials in teeth [5]. The moisture absorption and expansion of the matrix in the resin-based composite will lead to interface debonding and matrix cracking, which will accelerate the penetration and diffusion of moisture in the material. Therefore, the moisture absorption process of the composite is a self-accelerated vicious cycle [6]. The hygrothermal environment will affect the performance of advanced composites during use, so it is significant to research the mechanical properties of composites working in hygrothermal environments.

In recent years, many researchers have studied the mechanical properties of composites in hygrothermal environments and achieved some results. Ma et al. [7] measured the mechanical properties of composite laminates with defects using moisture absorption and compression tests. The impact of hygrothermal conditions on the moisture absorption performance, compressive strength, and failure mode of defective laminates has been analyzed. Almeida et al. [8] studied the compressive, tensile, in-surface, and interlayer shear properties of carbon fiber/epoxy composite laminates in hygrothermal conditions. After hygrothermal aging, it has been concluded that the shear modulus and strength of the samples decrease by about 38 and 30%, respectively. At the same time, it has been pointed out that the main damage mode of the samples is interfaced debonding. Chakraverty et al. [9] have studied shear specimens of the glass-fiber-reinforced epoxy composite subjected to three-point bend test in hygrothermal and hydrothermal conditionings.

^{*} Corresponding author: Shi Yan, Department of Engineering Mechanics, Harbin University of science and Technology, Harbin, China, e-mail: yanshi@hrbust.edu.cn

Modulus, interlaminar shear strength and stress/strain at rupture of materials under two conditions are obtained. Interlaminar shear strength is reduced by 25% after 90 days of hygrothermal conditioning and 23% after 120 days of hydrothermal conditioning. Rocha et al. [10] carried out quasi-static and fatigue experiments on glass/epoxy composite specimens after hygrothermal aging experiments with 4,800 h in water at 50°C. Compared with the experimental results at room temperature, the shear strength of the materials has been reduced by 36%, and the fatigue life has been shortened by three orders of magnitude. Xu et al. [11] carried out tension and compression tests of carbon fiber/epoxy composites samples under different hygrothermal conditions and discussed the influence of hygrothermal environments on the tensile and compressive performance of materials. At 130°C after moisture absorption, tensile and compressive strengths reduce 4 and 31%, respectively. Chao et al. [12] pointed out that there is an approximately linear relationship between the moisture absorption rate and the shear strength retention rate of the composites. As hygrothermal aging time increases, the cracks in the material develop from inland to layers, and finally, both cracks interweave to form reticular cracks. Xu et al. [13] carried out hygrothermal experiments on four types of T700-grade JH carbon fiber/bismaleimide resin (QY9611, 5,429, QY9512, and QY8911-4) composites under different hygrothermal conditions. By means of the study of the microstructure, chemical component, diffusion coefficient, and hygrothermal aging characteristics of composites have been analyzed. Feng et al. [14] investigated the moisture absorption performance of T700/3228 carbon-fiber-reinforced plastic laminates and analyzed the tensile and compressive properties of specimens under different hygrothermal conditions. The degradation mechanism of tensile and compressive performances has been further studied through microstructure characterization. Xie et al. [15] carried out the dry and wet cycle experiments of carbon fiber and epoxy resin at 25°C and 60% relative humidity. Experimental results show that the tensile and compressive performances of epoxy resin matrix are more sensitive to the hygrothermal condition compared with carbon fiber. Mansouri et al. [16] analyzed the mechanical properties such as ultimate stress, yield strength, and bending modulus of mixed short fiber/ woven composites under hygrothermal aging using threepoint bending tests. Experimental results show that aging time and temperature have a significant impact on the mechanical performances of materials. Behera et al. [17] carried out hygrothermal aging and fatigue tests on

carbon-fiber-reinforced polymer multidirectional composite laminates with two kinds of ply angles and investigated the effects of hygrothermal aging and fiber orientation upon glass transition temperature, Fourier transform infrared spectra, moisture diffusivity rate, and fatigue strength compared with the virgin properties.

As a kind of fiber-reinforced composites, 3D braided composites are applied in various fields because of overcoming many shortcomings of laminated composites, such as low interlayer shear strength, poor performance in the thickness direction, low impact toughness and damage tolerance, and so on. At present, researches on the mechanical properties of fiber-reinforced composites under hygrothermal environments mainly focus on laminated composites, but there are few reports on 3D braided composites. In consequence, it is significant to investigate the mechanical properties of 3D braided composites in a hygrothermal environment.

In this work, the hygrothermal aging tests of 3D five-directional braided composites with three braiding angles are conducted to extend to analyze the influence of moisture diffusion on fiber bundles and matrix from a micro perspective. By comparing the compressive experimental data of specimens after hygrothermal aging and at room temperature, the influence of moisture absorption percentage, water bath temperature, and aging time on the compressive performance of 3D five-directional braided composites is researched. The results of this paper provide a theoretical reference for the application of 3D braided composites in a hygrothermal environment.

2 Materials and methods

2.1 Materials

The 3D five-directional braided structure is an integral braided structure formed by introducing axial yarns in the braiding direction on the basis of the 3D four-directional braided structure. As shown in Figure 1, the specimen is the 3D five-directional carbon fiber/epoxy resin braided composites prepared by the Institute of Composite Materials of Tianjin University of Technology. The 3D five-directional braided composites are a periodic structure composed of many unit cells. Figure 2 illustrates 3D five-directional braided composite unit cell model. The matrix resin is TDE-86 epoxy resin, and the reinforced fiber is T700-12K carbon fiber produced by Toray Company of Japan. The diameter of carbon fiber monofilament is 7 µm.

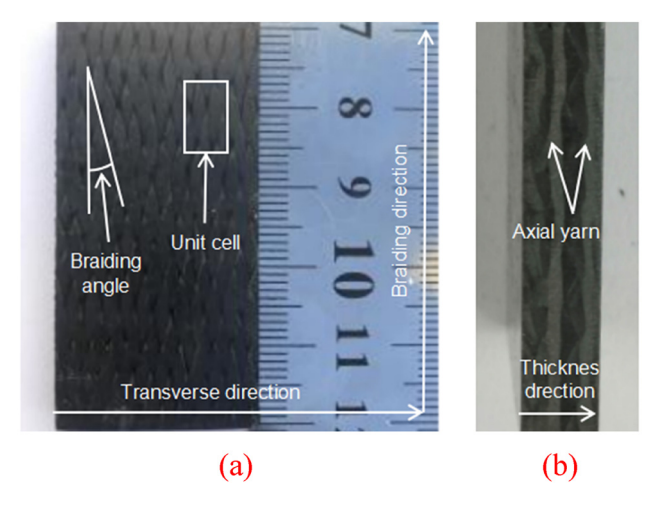


Figure 1: Specimen of 3D five-directional braided composite. (a) Front view; (b) side view.

The performances of component materials are shown in Table 1. The specimens adopt a four-step weaving process and then solidify them through the resin transfer molding process. The dimensions of all specimens are $50 \text{ mm} \times 24 \text{ mm} \times 5 \text{ mm}$. Three braiding angles (15, 25, and 35°) are adopted with the same fiber volume content of 58%.

2.2 Hygrothermal aging test method

Before hygrothermal conditioning, the samples were dried in a drying oven at 85°C until the engineering dry state. The hygrothermal aging tests were carried out according to the ASTM D5229M-2014 standard in three constant temperature water bath tanks at temperatures set to 40, 60, and 80°C, and the aging times were defined as 7, 15, 30, and 60 days, respectively. The samples were taken out every 24 h for weighing until the hygrothermal aging time was reached. According to braiding angle, water bath temperature, and aging time, specimens were divided into 39 groups and each group contains three samples. The experimental results took an average of three specimens.

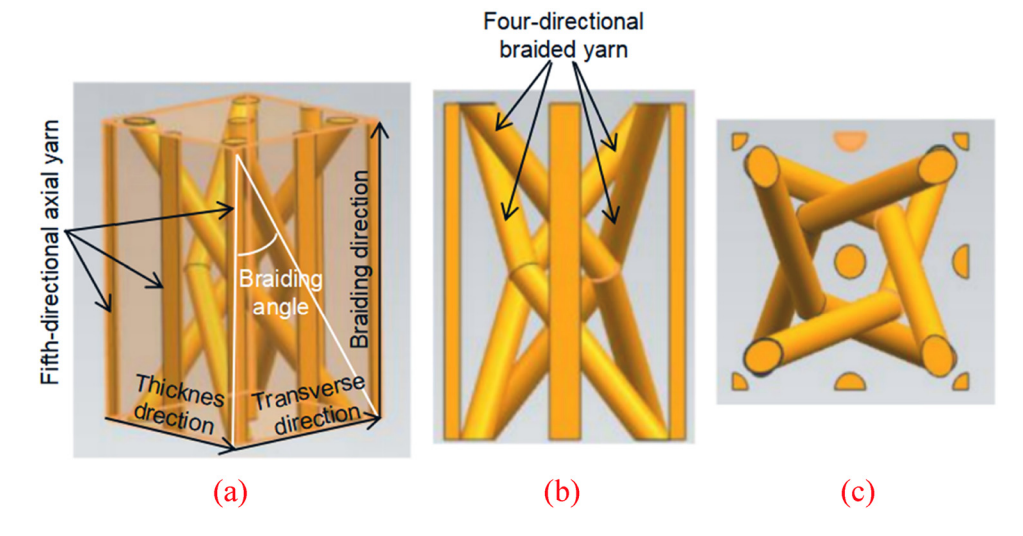


Figure 2: Representative unit cell of 3D five-directional braided composite. (a) Oblique view, (b) side view, and (c) vertical view.

Table 1: Performances of component materials

| Materials | <i>E</i> ₁₁ (GPa) | E ₂₂ (GPa) | G ₁₂ (GPa) | G ₂₃ (GPa) | μ ₁₂ |
|-----------------------|------------------------------|-----------------------|-----------------------|-----------------------|-----------------|
| TDE-86 epoxy resin | 3.45 | 3.45 | _ | _ | 0.35 |
| T700-12K carbon fiber | 215.6 | 17.21 | 12.92 | 9.3 | 0.3 |

^{*1 –} Braiding direction; 2 – transverse direction; 3 – thickness direction.

^{*}E₁₁ - Elastic modulus in braiding direction.

^{*}E22 - Elastic modulus in transverse direction.

 $[*]G_{12}$ – Shear modulus in 12-plane.

^{*} G_{23} - Shear modulus in 23-plane.

^{*} μ_{12} – Poisson's ratio in 12-plane.

The surface morphologies of the specimens before and after the hygrothermal aging experiments were taken by microstructural examination (SEM, Apreo, Thermo Scientific, USA) with a magnification of 1,000.

2.3 Compression test method

According to ASTM D6641M- 2014, compression tests of 3D five-directional braided composites after hygrothermal aging were carried out on the INSTRON3382. The loading rate was 0.5 mm min⁻¹, marking two points on the central axis of the specimen, and the strain of the sample was tested by locking the marker by the infrared RF meter. The compressive experiment process is shown in Figure 3. The ultimate loads of specimens can be measured by tests, and compressive strength is defined as the ultimate load divided by the cross-sectional area of the specimen.

3 Experimental results and discussion

3.1 Analysis of hygrothermal aging test

According to the data measured by the experiments, the weight gain rate of each specimen is calculated by equation (1):

$$M_t = \frac{W_t - W_0}{W_0} \times 100\%. \tag{1}$$

where M_t is the moisture absorption percentage and W_t (g) is the weight of the sample when the aging time is t;

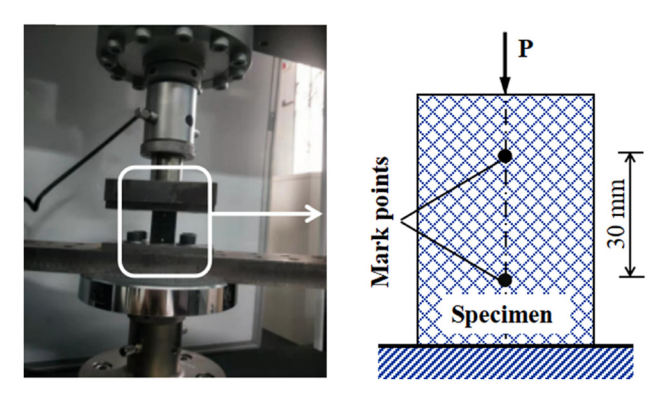


Figure 3: Illustration of a compression test.

 W_0 (g) is the initial weight of the sample before the hygrothermal aging experiment.

The surface morphologies of the specimens before and after the hygrothermal aging experiments were analyzed by SEM as shown in Figure 4. Under the condition of no hygrothermal aging at room temperature, fiber and matrix in the material are tightly bonded and massive resin is attached to the surface of the fiber. With the increase in water bath temperature, part of carbon fibers are completely debonded from the matrix because of the difference in expansion rates between matrix and fiber, and this reason leads to cracks inside the material. Cracks provide some channels for moisture diffusion into the interior of the material, which reduces the compressive performances of composites and shortens the service life. As shown in Figure 4, with the increase in water bath temperature, debonding between matrix and fiber becomes more and more obvious. Hence, the hygrothermal aging conditions have a significant influence on the internal structure of braided composites.

Figure 5(a)–(c) gives the relationship between hygrothermal aging time and moisture absorption percentage of 3D five-directional braided composites under three water bath temperatures of 40, 60, and 80°C. The whole hygroscopic process is roughly divided into two phases as shown in Figure 5. In the first phase, all specimens show a trend of rapid weight gain. The moisture absorption percentage in this phase is approximately proportional to the square root of time, so it conforms to Fick's law. In the second phase, with the continuous extension of aging time, the moisture absorption percentage rises slowly and tends to be balanced, indicating that the specimen gradually reaches a hygroscopic saturation state and the weight has hardly changed.

In Figure 5(a)-(c), it can be shown that the time of reaching the hygroscopic saturation state of samples with different braiding angles is almost the same at an equal temperature. At the water bath temperature of 40, 60, and 80°C, the time for specimens to reach hygroscopic saturation is 50, 41, and 21 days, respectively. With increasing temperature, the accelerated diffusion of water molecules leads to an increase in the permeability of the fiber-matrix interface. Hence, the moisture absorption percentage of samples with the same braiding angle at 80°C is significantly higher than results at 40 and 60°C. At 80°C, the moisture absorption percentages in the saturation state of samples with braiding angles of 15, 25, and 35° are 3.21, 2.66, and 2.26%, respectively. From Figure 5(a)-(c), it is shown that the moisture absorption percentage under the same temperature of

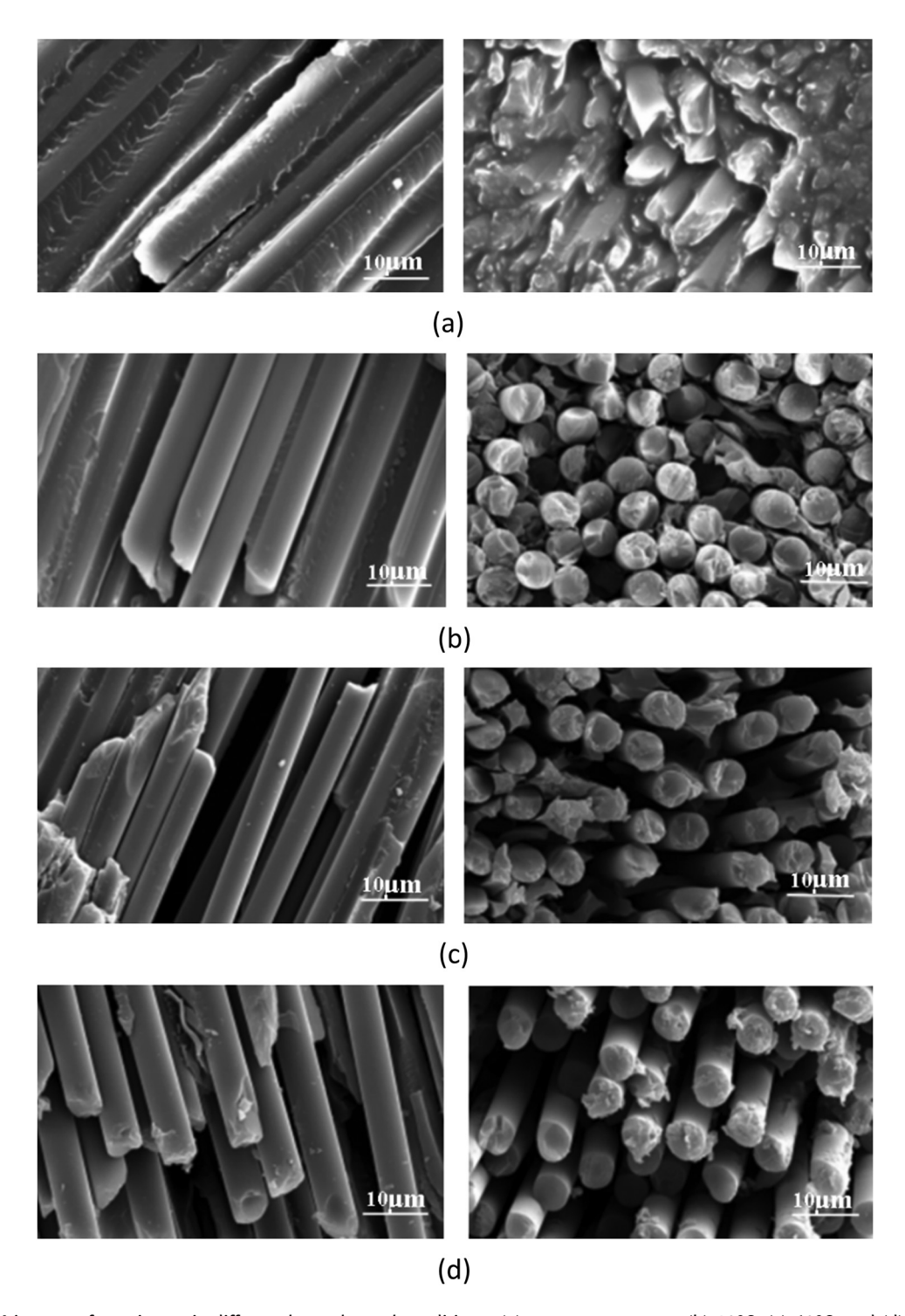


Figure 4: SEM images of specimens in different hygrothermal conditions: (a) room temperature, (b) 40°C, (c) 60°C, and (d) 80°C.

specimens with a braiding angle of 15° is larger than those with braiding angles of 25 and 35°. This is because of the larger braiding angle, the denser arrangement of the fibers, and the greater curvature of the fiber bundle, which hinder the diffusion of water molecules in the material.

3.2 Compressive properties of materials under hygrothermal environment and room temperature

The load-displacement curves of specimens are obtained using compression tests before and after hygrothermal

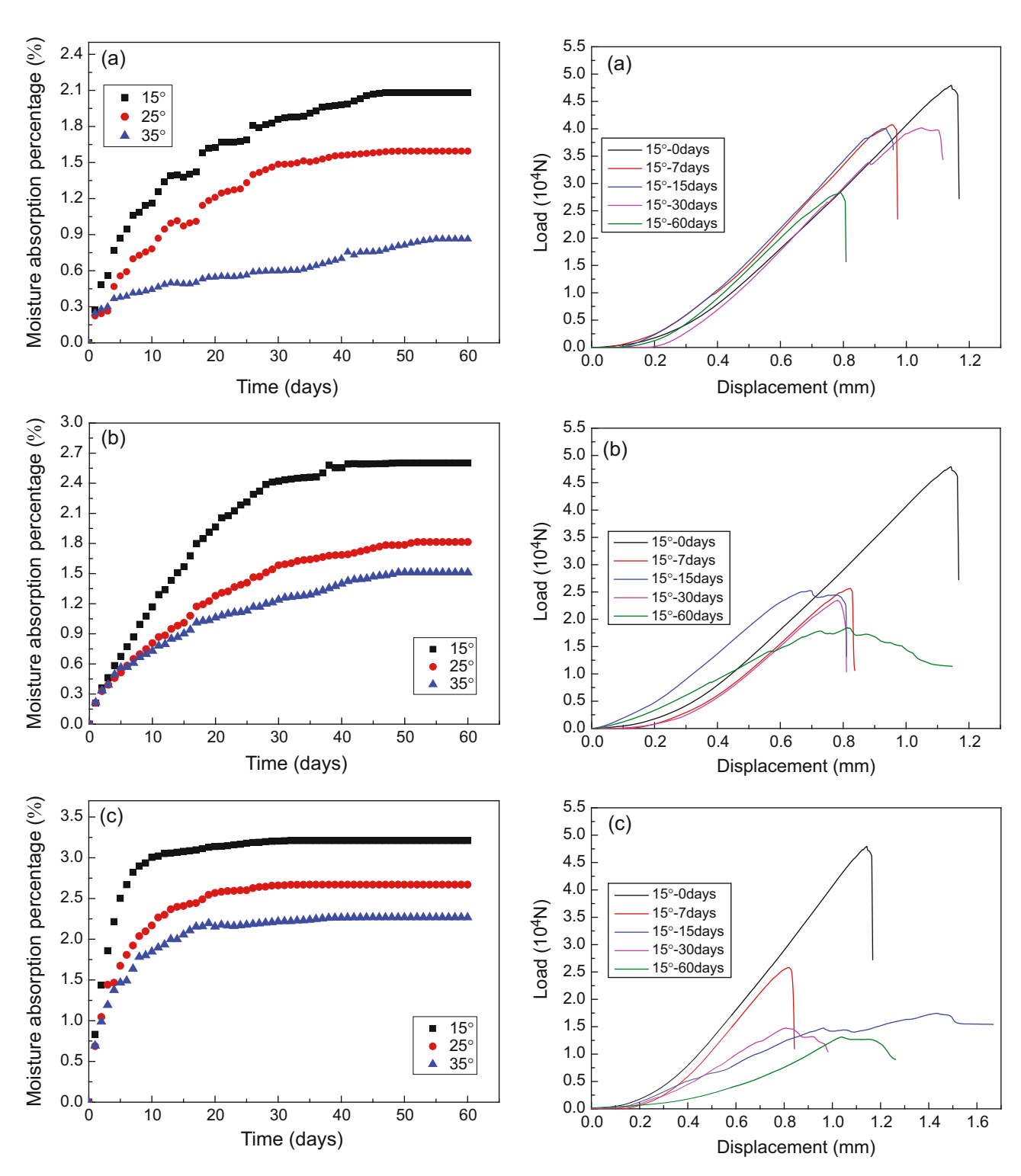


Figure 5: The moisture absorption percentage curves of 3D braided composites under different hygrothermal conditions. (a) 40°C, (b) 60°C, and (c) 80°C.

Figure 6: Load-displacement curves of specimens with 15° under different hygrothermal aging conditions. (a) 40° C, (b) 60° C, and (c) 80° C.

aging, as shown in Figures 6–8. Each picture shows that the ultimate load of specimens after hygrothermal aging has been reduced to varying degrees compared with

samples that are at the dry condition of room temperature. At a specified braiding angle, the ultimate load shows a downward trend with the rising water bath

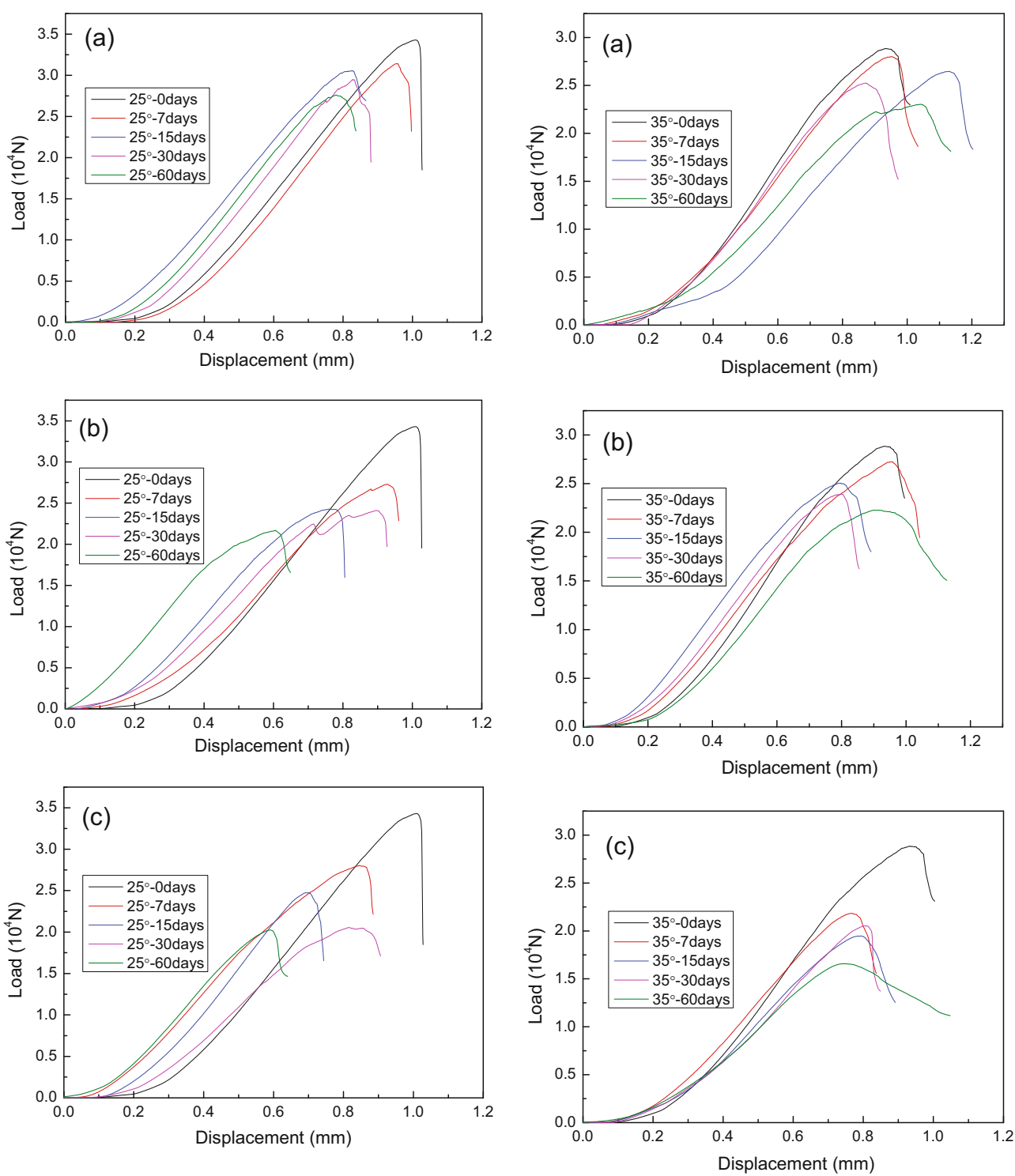


Figure 7: Load-displacement curves of specimens with 25° under different hygrothermal aging conditions. (a) 40° C, (b) 60° C, and (c) 80° C.

Figure 8: Load-displacement curves of specimens with 35° under different hygrothermal aging conditions. (a) 40°C, (b) 60°C, and (c) 80°C.

temperature and aging time. To specimens with different braided angles, the influence of the hygrothermal environment on the ultimate load shows different characteristics. In Figures 6–8, compared with room temperature,

the ultimate load of samples with braiding angles of 15, 25, and 35° decreased 72.2, 54, and 42.9% with increasing temperature from 40 to 80°C. Thus, the impact of water

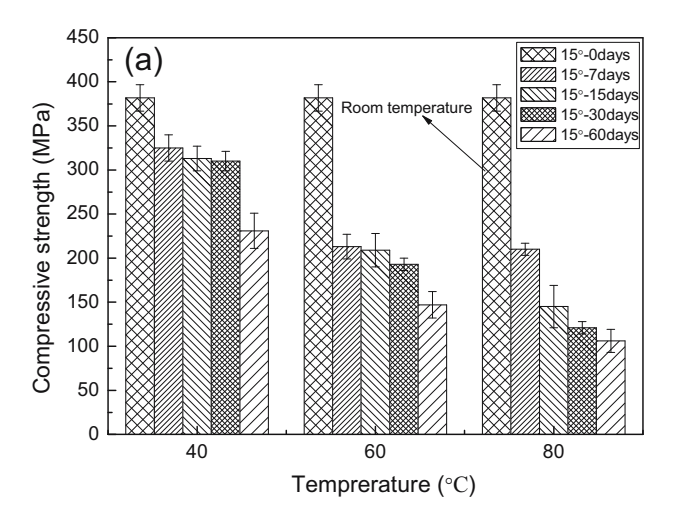
bath temperature and aging time on the ultimate load of specimens with 15° is greater than those with 25 and 35°.

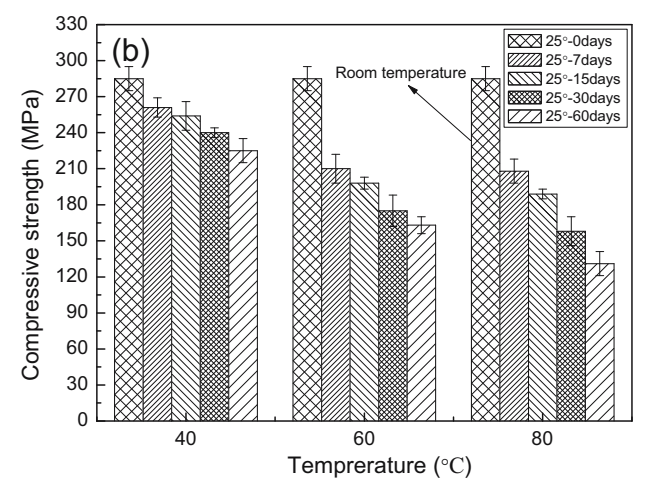
In addition, Figure 6(a)–(c) shows that some curves of the specimens with a braiding angle of 15° are linear before reaching the ultimate load and dropped rapidly after reaching the maximum. These curves show an obvious brittle failure characteristic. With the increase in temperature and aging time, a few curves gradually present a nonlinear trend, such as a curve (15°, 60 days) in Figure 6(b), curves (15°, 15 days; 15°, 30 days; 15°, 60 days) in Figure 6(c). It indicates there is an obvious yield phenomenon in these curves which is characterized by significant plastic failure. Figure 6 shows hygrothermal environment can change the failure mechanism of materials with a braiding angle of 15°. In Figures 7-8, the shape of the curves does not change significantly with the increase in temperature and aging time, indicating that the failure mechanism of the specimens with braid angles of 25 and 35° has no qualitative change before and after hygrothermal aging.

Figure 9(a)–(c) give the compressive strength of specimens at room temperature and under different hygrothermal conditions. The compressive strength of materials reduces with the increase in braiding angle, water bath temperature, and aging time. Histograms indicate that the hygrothermal environment has a greater impact on the compressive strength of specimens with 15° than those at 25 and 35°. Under temperature of 80°C and aging time of 60 days, the compressive strength of specimens with 15, 25 and 35° decreased 72.2, 54, and 42.9% respectively.

Figure 10(a)–(c) shows the compressive modulus of specimens at room temperature and under different hygrothermal conditions. The compressive modulus of materials reduces with the increase in braiding angle, water bath temperature, and aging time. For the specimens with braiding angles of 25°C and 35°, the hygrothermal environment has little effect on the compressive modulus and variation in compressive modulus before and after hygrothermal aging is small. However, the influence of the hygrothermal environment on the compressive modulus of specimens with a braiding angle of 15° increases with rising temperature. Under temperature of 80°C and aging time of 60 days, the compressive modulus of specimens with 15, 25, and 35° decreased 82.7, 28.2, and 24.8%, respectively.

Tables 2 and 3 give moisture absorption percentage and compressive strength and modulus of samples with three braiding angles at an aging time of 60 days. Moisture absorption percentage increases, and compressive strength and modulus decrease with the increase in





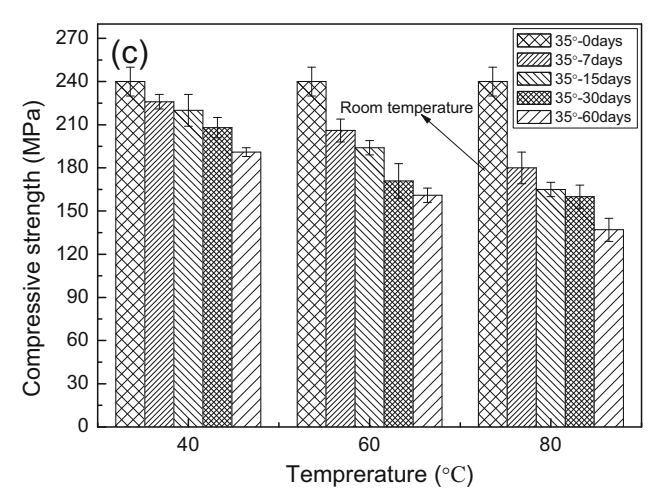
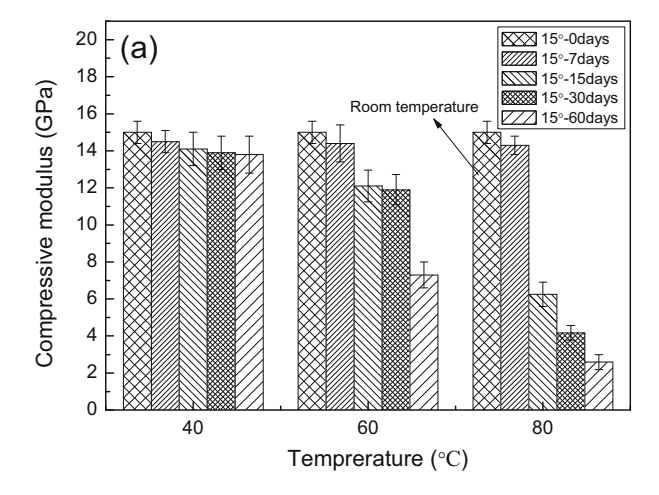
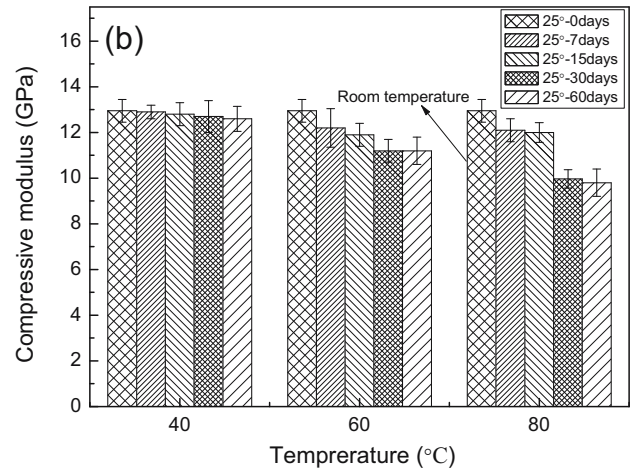


Figure 9: Compressive strength of specimens with different braiding angles in hygrothermal conditions. (a) 15°C, (b) 25°C, and (c) 35°C.

temperature under the same braiding angle. Comparing the data of three braiding angles, a very interesting conclusion can be drawn. At room temperature, compressive strength and modulus decrease with the rising braiding





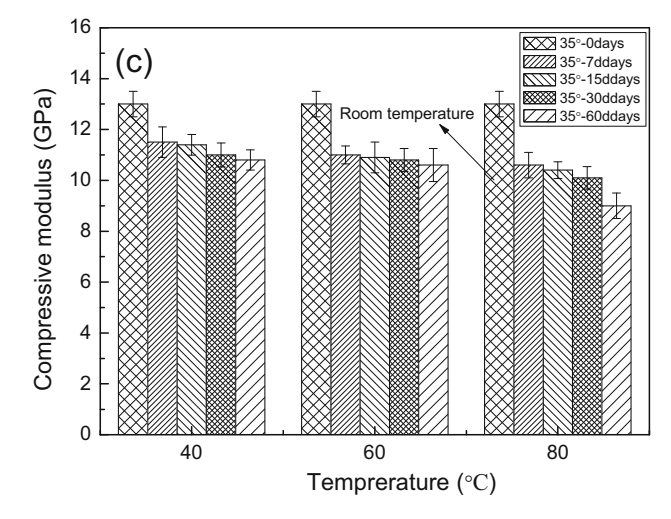


Figure 10: The compressive modulus of specimens with different braiding angles in hygrothermal conditions. (a) 15°C, (b) 25°C, and (c) 35°C.

angle. But with the increase in temperature and moisture absorption percentage, the conclusion is the opposite. At 40°C, the moisture absorption percentages of specimens with 15, 25, and 35° are 2.08, 1.59, and 0.86%, respectively.

At this temperature, the retention ratios of compressive strength for three types of specimens are 60.6, 78.9, and 79.6%, respectively; at the same time, the retention ratios of compressive modulus are 92.7, 91, and 86.6%, respectively. It indicates that the moisture absorption percentage of specimens has a greater impact on strength than on modulus at 40°C. While at 80°C, the moisture absorption percentages of specimens with 15, 25, and 35° are 3.21, 2.66, and 2.26%, respectively. At this temperature, the retention ratios of compressive strength for three types of specimens are 27.8, 46, and 57.1% respectively; meanwhile, the retention ratios of compressive modulus are 17.3. 71.8, and 75.2%, respectively. It shows that the moisture absorption percentage of specimens also has a large influence on strength and modulus at 80°C. Figure 4 shows the moisture absorption percentage decreases with the increase in braiding angle at the same temperature and aging time. So the moisture absorption percentage of specimens with a braiding angle of 15° is greater than those with 25 and 35° at the same hygrothermal condition. Tables 2 and 3 indicate the retention ratios of compression strength and modulus of specimens with a braided angle of 15° at 80°C are 27.8 and 17.3%, far lower than those with 25 and 35°. These data show two problems. First, the value of moisture absorption percentage determines the degree of its influence on the mechanical properties of the material. The greater the moisture absorption percentage, the lower the retention ratio of compressive strength and modulus. The other is that the hygrothermal environment has a greater impact on the specimens with a braiding angle of 15°.

Figure 11(a)–(c) shows the compressive damage images (28 mm \times 38 mm, font size: 8) of specimens with three braided angles without hygrothermal aging at room temperature. The images indicate the main failure mode of specimens with three braiding angles is fiber fracture, accompanied by matrix cracking and interface debonding. Interface debonding grew gradually as the braiding angle increases.

Figure 12(a)–(c) indicates the compressive damage images ($28 \text{ mm} \times 38 \text{ mm}$, font size: 8) of specimens with three braided angles under a water bath temperature of 80° C and an aging time of 30 days. Compared with Figure 11, it can be found that the damage modes before and after hygrothermal aging are similar, but the degree of damage is aggravated. The interfacial adhesion between fiber and matrix is weakened by the influence of the hygrothermal environment, which leads to a significant increase in the interface debonding.

Figure 13 indicates the compressive damage images $(21.6 \text{ mm} \times 16.8 \text{ mm}, \text{ font size: 8})$ of specimens with a

Table 2: Moisture absorption percentage and compressive strength at aging time of 60 days

| Braiding angle (°) | Room temperature | 40°C | | 60°C | | | 80°C | | | |
|-----------------------|------------------|---------|----------|----------|---------|----------|----------|---------|----------|----------|
| | CS (MPa) | MAP (%) | CS (MPa) | CSRR (%) | MAP (%) | CS (MPa) | CSRR (%) | MAP (%) | CS (MPa) | CSRR (%) |
| 15 | 381 | 2.08 | 231 | 60.6 | 2.60 | 147 | 38.6 | 3.21 | 106 | 27.8 |
| 25 | 285 | 1.59 | 225 | 78.9 | 1.81 | 163 | 57.2 | 2.66 | 131 | 46.0 |
| 35 | 240 | 0.86 | 191 | 79.6 | 1.51 | 161 | 67.1 | 2.26 | 137 | 57.1 |

^{*}MAP, Moisture absorption percentage; CS, compressive strength; and CSRR, compressive strength retention ratio.

Table 3: Moisture absorption percentage and compressive modulus at aging time of 60 days

| Braiding angle (°) | Room temperature | 40°C | | 60°C | | | 80°C | | | |
|-----------------------|------------------|---------|----------|----------|---------|----------|----------|---------|----------|----------|
| | CM (GPa) | MAP (%) | CM (GPa) | CMRR (%) | MAP (%) | CM (GPa) | CMRR (%) | MAP (%) | CM (GPa) | CMRR (%) |
| 15 | 15.0 | 2.08 | 13.9 | 92.7 | 2.60 | 7.3 | 48.7 | 3.21 | 2.59 | 17.3 |
| 25 | 13.3 | 1.59 | 12.1 | 91.0 | 1.81 | 10.2 | 76.7 | 2.66 | 9.4 | 71.8 |
| 35 | 12.9 | 0.86 | 11.2 | 86.8 | 1.51 | 10.6 | 82.2 | 2.26 | 9.7 | 75.2 |

^{*}CM, Compressive modulus; CMRR, compressive modulus retention ratio.

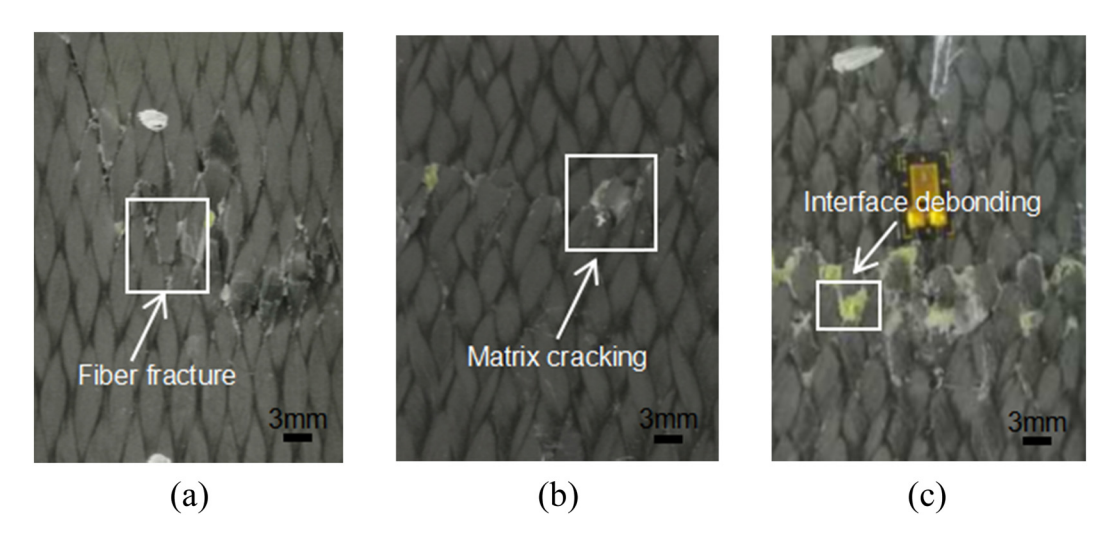


Figure 11: Damage images of compressive specimens with three braiding angles under room temperature. (a) 15°, 0 days; (b) 25°, 0 days; and (c) 35°, 0 days.

braiding angle of 15° at three temperatures (40, 60, and 80°C) for two aging times of 7 and 60 days. Comparing the pictures of the aging time of 7 days, damage modes of materials are similar, such as fiber fracture, matrix cracking, and interface debonding, and damage degree increases with the increase in temperature. This is because the failure modes of fiber and matrix do not change qualitatively due to a short aging time. For the aging time of 60 days, damage also increases significantly as temperature increases, but at a temperature of 80°C, the specimens show matrix pulverization which indicates the

failure mechanism of the matrix has changed. On the one hand, matrix pulverization will reduce the support of the matrix to fibers. On the other hand, the internal structure of samples with a braiding angle of 15° is not tight enough. Both factors lead to a great decrease in the mechanical properties of specimens with a braiding angle of 15° at 80°C. For the specimens with braiding angles of 25 and 35°, although the matrix will also pulverize at 80°C, because of the tight internal structure, the mechanical properties do not drop as much as the specimen with a braiding angle of 15°. The analysis

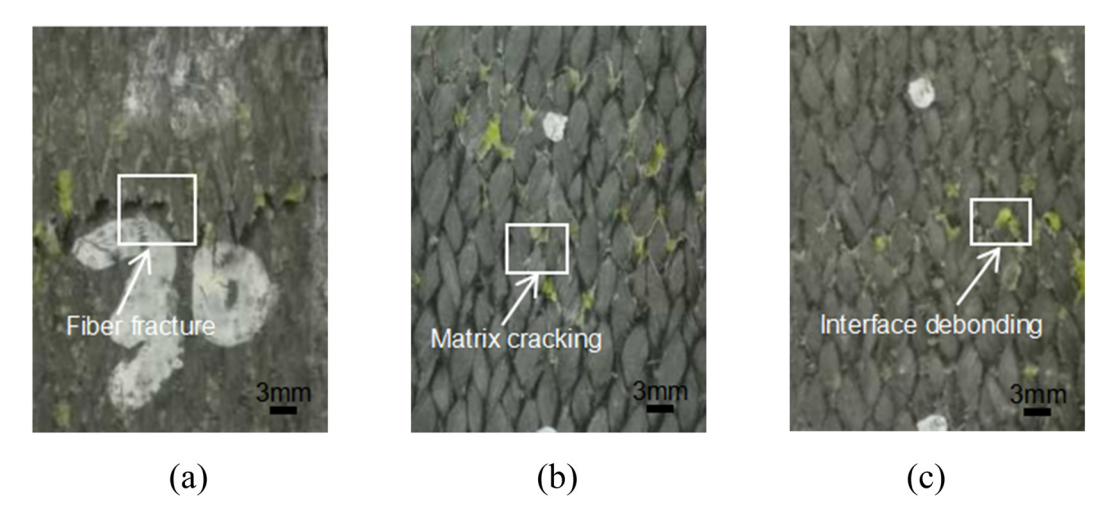


Figure 12: Damage images of compressive specimens with three braiding angles in the hygrothermal environment: (a) 15-80°C-30 days; (b) 25-80°C-30 days; and (c) 35-80°C-30 days.

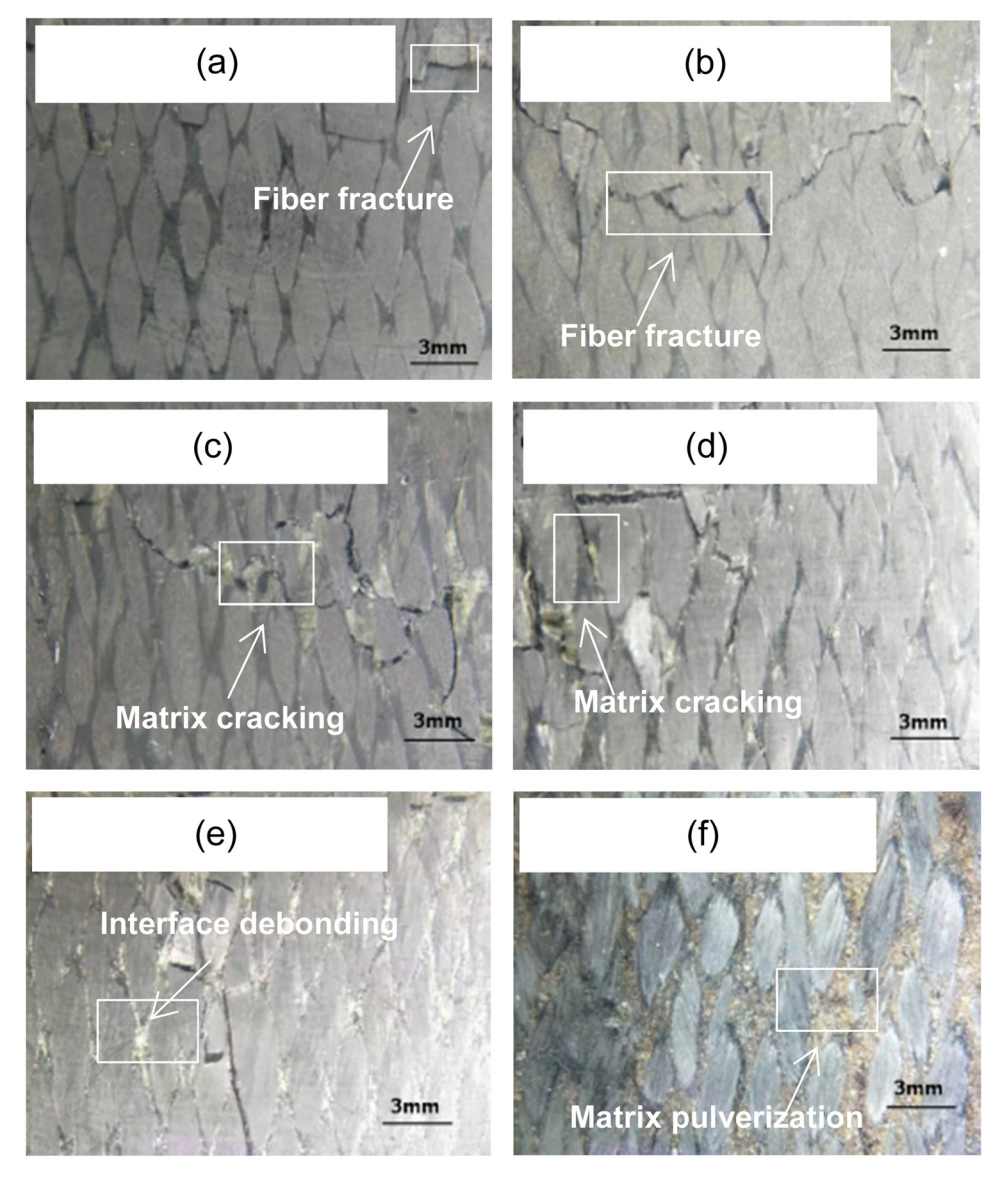


Figure 13: Damage images of compressive specimens with the braiding angle of 15° under different hygrothermal aging conditions: (a) $15-40^{\circ}C-7$ days; (b) $15-40^{\circ}C-60$ days; (c) $15-60^{\circ}C-7$ days; (d) $15-60^{\circ}C-60$ days; (e) $15-80^{\circ}C-7$ days; (f) $15-80^{\circ}C-60$ days.

above of the failure mechanism is consistent with what is presented in Figures 6 and 9(a).

4 Conclusions

- (1) The moisture absorption percentage of 3D five-directional braided composites increases with the increase in water bath temperature and aging time and decreases with the increase in braiding angle.
- (2) Compressive load-displacement curves shows ultimate load after hygrothermal aging declines with the increase in braiding angle, water bath temperature, and aging time. Compared with the other braiding angles, hygrothermal environment has the greatest influence on the mechanical behavior of specimens with a braiding angle of 15°. As the temperature increases from 40 to 80°C, the failure mode of the specimen with the braiding angle of 15° gradually transitions from brittle fracture to plastic yielding.
- (3) Compressive strength and modulus of 3D five-directional braided composites decrease as braiding angle, water bath temperature, and aging time increase. The effect of hygrothermal environment on the compressive strength and modulus of materials gradually decreases as braiding angle increases. The greater the moisture absorption percentage, the lower the retention ratio of compressive strength and modulus. At room temperature, compressive strength and modulus decrease with the rising braiding angle. But at a temperature of 80°C, the conclusion is opposite.
- (4) After hygrothermal aging, damage of materials has intensified and interface debonding between fiber and matrix has increased significantly. The experimental results of two aging times of the specimens with a braiding angle of 15° were compared. For aging time of 7 days, damage modes of specimens are similar and damage degree increases with the increase in temperature. For aging time of 60 days, matrix pulverization at 80°C and non-tight internal structure lead to a great decrease in the mechanical properties of materials.

Acknowledgments: This study has been funded by the National Natural Science Foundation of China (Grant No. 11972140).

Conflict of interest: The authors state no conflict of interest.

References

- [1] Li DS, Lu ZX, Jiang N, Fang DN. High strain rate behavior and failure mechanism of three-dimensional five-directional carbon/phenolic braided composites under transverse compression. J Compos Part B-Eng. 2011;42(2):309-17.
- [2] Ansar M, Wang X, Zhou C. Modeling strategies of 3D woven composites: A review. J Compos Struct. 2011;93(8):1947-63.
- [3] Golewski GL. Physical characteristics of concrete, essential in design of fracture-resistant, dynamically loaded reinforced concrete structures. J Mat Des Process Comm. 2019;1(5):e82.
- [4] Golewski GL, Szostak B. Application of the C-S-H phase nucleating agents to improve the performance of sustainable concrete composites containing fly ash for use in the precast concrete industry. J Mater. 2021;14:6514.
- [5] Alvarez VA, Vazquez A. Effect of water sorption on the flexural properties of a fully biodegradable composite. J Compos Mater. 2004;38:1165–82.
- Guo M, Ling X. Study on hygrothermal ageing mechanisms of aerospace structural composites. J Aerosp Mater Technol. 2002;32:51-4.
- [7] Ma SH, Wang YG, Hui L, Fei BQ. Compressing property of composite laminate with hole in hygrothermal environment. J Aerosp Mater Technol. 2015;6:66-70.
- [8] Almeida J, Souza S, Botelho EC, Amico SC. Carbon fiber-reinforced epoxy filament-wound composite laminates exposed to hygrothermal conditioning. J Mater Sci. 2016;51:4697-708.
- [9] Chakraverty AP, Mohanty UK, Mishra SC, Biswal BB. Effect of hydrothermal immersion and hygrothermal conditioning on mechanical properties of GRE composite. Iop Conf. 2017;178:012013.
- [10] Rocha IBCM, Raijmaekers S, Nijssen RPL, Van der Meer FP, Sluys LJ. Hygrothermal ageing behaviour of a glass/epoxy composite used in wind turbine blades. J Compos Struct. 2017;174:110–22.
- [11] Xu L, Fei BQ, Ma SH, Hui L, Huang GD. Tensile and compress property of composite laminate in hygrothermal environment. J Mater Eng. 2018;46:124–30.
- [12] Chao S, Liu L, Zhao Z, Guan Y, Chen W. Effect of hygrothermal aging on interlaminar shear strength of T700/TDE-85 composite. J Mater Mech Eng. 2018;42:62-6.
- [13] Xu WW, Wen YY, Gu YZ, Li B, Tu JY, Zhang ZG. Hygrothermal property of domestic carbon fiber/bismaleimide resin composites for aeronautic application. J B Univ Aeronaut Astronaut. 2020;46:86–94.
- [14] Feng Z, Mou H, Xie J, Gong T. Hygrothermal environment effects on mechanical properties of T700/3228 CFRP laminates. J Mater Test. 2019;61:857-63.
- [15] Xie J, Lu Z, Guo Y, Huang Y. Durability of CFRP sheets and epoxy resin exposed to natural hygrothermal or cyclic wet-dry environment. J Polym Compos. 2019;40:553-67.
- [16] Mansouri L, Djebbar A, Khatir S, Wahab MA. Effect of hygrothermal aging in distilled and saline water on the mechanical behaviour of mixed short fibre/woven composites. Compos Struct. 2019;207:816-25.
- [17] Behera A, Dupare P, Thawre MM, Ballal A. Effects of hygrothermal aging and fiber orientations on constant amplitude fatigue properties of CFRP Multidirectional composite laminates. Int J Fatigue. 2020;136:105590.